

Effect of Regional Marine Cloud Brightening Interventions on Climate Tipping Points

Haruki Hirasawa¹, Dipti Hingmire¹, Hansi Singh¹, Philip J. Rasch², Peetak Mitra^{3,4}

¹School of Earth and Ocean Sciences, University of Victoria, Victoria, BC, Canada

²Department of Atmospheric Sciences, University of Washington, Seattle, WA, USA

³Palo Alto Research Center, Palo Alto, CA, USA

⁴Excarta, San Francisco, CA, USA

Key Points:

- The magnitude and pattern of the Marine Cloud Brightening (MCB) climate impact depends strongly on the location of the intervention
- The MCB impact generally indicates reduced tipping point risk overall, but certain intervention patterns may exacerbate some tipping points
- We find MCB impacts that have qualitative similarities to prior work, but we find discrepancies that suggest key inter-model uncertainties

Corresponding author: Haruki Hirasawa, hhirasawa@uvic.ca

Abstract

It has been proposed that increasing greenhouse gas (GHG)-driven climate tipping point risks may prompt consideration of Solar Radiation Modification (SRM) climate intervention to reduce those risks. Here, we study marine cloud brightening (MCB) SRM interventions in three subtropical oceanic regions using the Community Earth System Model 2 (CESM2) experiments. We assess the response of tipping point-related metrics to estimate the extent to which such interventions could reduce tipping point risk. Both the pattern and magnitude of the MCB cooling depend strongly on location of the MCB intervention. We find the MCB cooling effect reduces tipping point risk overall; however, the distinct pattern effects of MCB versus GHG means it is an imperfect remedy. Indeed, if MCB is applied in certain oceanic regions, it may exacerbate some tipping point risks. It is therefore crucial to carefully assess the potential remote teleconnected response to MCB interventions to reduce unintended climate impacts.

Plain Language Summary

Marine Cloud Brightening (MCB) is a proposed technology where sea salt particles would be sprayed into clouds over oceans to increase scattering of sunlight by the clouds, thus cooling the surface. If greenhouse gas warming continues to intensify, solar radiation modification (SRM) technologies like MCB might be considered as methods to avoid the potentially devastating climate changes, such as climate system tipping points. Here, we analyse the MCB impact on a set of tipping point-related metrics in a set state-of-the-art climate model experiments. Our experiments indicate that MCB reduces risks for most tipping points considered here, such as by reducing sea ice loss and increasing Atlantic overturning circulation. However, the MCB impact strongly depends on the location of the intervention, meaning the pattern of MCB deployment must be carefully considered to avoid unintended effects on regional climate.

1 Introduction

Current net-zero pledges are projected to cause approximately 2C of warming above preindustrial (Meinshausen et al., 2022), a level of warming that at which there is a substantial risk of crossing some climate tipping point thresholds McKay et al. (2022). Thus, unless more aggressive mitigation is undertaken, projected emissions could induce self-perpetuating regional and global climate changes that would hinder future efforts to re-

turn the climate to its past state via greenhouse gas (GHG) reductions. Given that we may fail to fulfil mitigation commitments, that climate sensitivity may be higher than expected, and/or that some tipping points may be more sensitive than expected, climate interventions may become the only sufficiently rapid method to avert catastrophic impacts. One class of climate intervention methods, known as solar radiation modification (SRM; also called solar geoengineering), has been proposed as a means to reduce the probability of tipping points as these methods are able rapidly reduce surface temperatures (The Royal Society, 2009; National Academies of Sciences, Engineering, and Medicine, 2021; United Nations Environment Programme, 2023). However, Earth System Model (ESM) studies suggest SRM interventions are imperfect methods for counteracting GHG-induced climate changes. Thus, it is crucial to judiciously evaluate the extent to which SRM could indeed reduce tipping point risks relative to a warming world.

Here we use a state-of-the-art ESM to assess one proposed SRM technique, marine cloud brightening (MCB), and its potential effects on the risk of crossing tipping point thresholds. MCB is a proposed method intended to increase the reflectivity of marine boundary layer clouds by emitting sea salt aerosol in certain oceanic regions. These emissions would increase cloud condensation nuclei (CCN) concentrations, increasing cloud droplet number concentrations (CDNC), and decreasing cloud droplet radii. This would increase the scattering of sunlight back to space and ultimately cool surface temperatures (Latham, 2002; Latham et al., 2012). These changes in CDNC can also induce changes in cloud water amount and cloud lifetime that can modulate the CDNC brightening effect, though optimized MCB strategies would be designed to avoid aerosol injections where these responses would substantially offset CDNC brightening (Wood, 2021). MCB is expected to be most effective in oceanic regions with extensive shallow stratocumulus cloud decks, which are sensitive to aerosol perturbations (Rasch et al., 2009; Latham et al., 2012).

In contrast to stratospheric aerosol injections which cause forcing over broad zonal bands (Tilmes et al., 2017), cloud responses to MCB injections are highly localized due to the short atmospheric lifetime of tropospheric aerosols and their impacts on cloud properties. The associated radiative response to MCB-induced cloud changes (termed MCB forcing hereafter) will also be localized (Latham et al., 2012). Thus, there are many different possible MCB forcing patterns with differing regional climate impacts which reduce the GHG impacts to varying degrees. Because much of MCB impact on climate will be remote from the MCB forcing regions themselves, there may be unintended telecon-

nected MCB climate impacts (Diamond et al., 2022). Thus, ESM representation of these teleconnections and the general circulation response are important considerations when assessing the feasibility of MCB interventions.

Past studies of MCB climate impacts have taken two main approaches. The first, exemplified by the Geoengineering Model Intercomparison Project MCB experiments, imposes uniform MCB perturbations over all oceans (Latham et al., 2008; Bala et al., 2011; Kravitz et al., 2013; Stjern et al., 2018; Duan et al., 2018) or over low-latitude oceans (Alterskjær et al., 2013; Muri et al., 2018). The second imposes MCB perturbations in regions with high concentrations of marine low clouds, which are more susceptible to aerosols and are typically found in subtropical regions at the eastern boundaries of oceanic basins (Rasch et al., 2009; Jones et al., 2009; Korhonen et al., 2010; Partanen et al., 2012; Hill & Ming, 2012; Stuart et al., 2013). The former protocol is more easily compared with stratospheric aerosol injection, a more extensively studied SRM technology, and more easily compared across ESMs. However, here we consider the latter protocol, as in practice MCB interventions are more likely to be focused in those regions in which sea salt emissions would most efficiently achieve cooling.

In particular, we use a protocol similar to those used by Jones et al. (2009) and Hill and Ming (2012). In these studies, MCB perturbations are applied the three regions most susceptible to aerosol increases (the subtropical Northeast Pacific - NEP, Southeast Pacific - SEP, and Southeast Atlantic - SEA). Both studies showed substantial differences in the global mean and pattern of climate response to MCB depending on which region is perturbed. These studies used Coupled Model Intercomparison Project 3 (CMIP3) generation models and consequently lack many of the improvements made in ESMs since. Thus, our ESM experiments provide an updated analysis of the MCB forcing mean climate responses in the three regions using a state-of-the-art CMIP6-generation ESM and provide a novel investigation of MCB effect on key climate tipping point metrics (TPM).

2 Methods

Our experiments are conducted using the Community Earth System Model 2 (CESM2; Danabasoglu et al., 2020). MCB forcing is approximated by prescribing the in-cloud liquid CDNC as a constant value at all vertical levels over ocean grid points in the Southeast Pacific (SEP - 30S to 0, 110W to 70W), Northeast Pacific (NEP - 0 to 30N, 150W

to 110W), and Southeast Atlantic (SEA - 30S to 0, 25W to 15E). As in previous work (Rasch et al., 2009; Jones et al., 2009), we use this method to avert uncertainties in the representation of sea salt aerosol generation and conversion to cloud droplets. That is, we assume sea salt injections will increase CDNC as hypothesized and study the climate responses of such cloud perturbations.

We specify the strength of the CDNC increase in the three regions (SEP, NEP, and SEA) such that the MCB effective radiative forcing (ERF) is -1.8Wm^{-2} , approximately half the ensemble mean forcing due to a doubling of CO_2 (Smith et al., 2018). Using fixed SST simulations, we find prescribing CDNC to 600cm^{-3} in the three regions achieves this with an ERF of $-1.9 \pm 0.1\text{Wm}^{-2}$ (2-standard error uncertainty). The forcing is largely confined to the perturbed regions and is dominated by the cloud shortwave effect (Fig. 1a). If we set CDNC to 600cm^{-3} in each of the regions individually, we find ERFs of $-0.7 \pm 0.1\text{Wm}^{-2}$ for the SEP, $-0.6 \pm 0.1\text{Wm}^{-2}$ for the NEP, and $-0.5 \pm 0.1\text{Wm}^{-2}$ for the SEA. The sum of ERFs from CDNC perturbation each region individually is approximately equal to the ERF from CDNC perturbations in all three regions simultaneously, and we do not find evidence of forcing non-linearity (in contrast to Jones et al., 2009).

We assess the MCB climate response with coupled CESM2 experiments wherein we use a SSP2-4.5 baseline forcing and set CDNC to 600cm^{-3} in all three regions simultaneously (ALL MCB) and each region separately (SEP, NEP, SEA) from 2015 to 2064. SSP2-4.5 is chosen as the baseline scenario following GeoMIP (Kravitz et al., 2015) and ARISE-SAI (Richter et al., 2022), which assessed SSP2-4.5 to be the most suitable policy relevant emission scenario. Three ensemble members are simulated in each MCB forcing case. Historical baseline data is obtained from the CESM2 Large Ensemble historical smoothed biomass burning experiments (BMB; see Rodgers et al., 2021). The coupled CESM2 experiments we use are summarized in Table 1. Statistical significance is tested using the Student's t-test with a p -value threshold as the lesser of $p < 0.05$ and the false discovery rate p_{fdr} for $\alpha = 0.1$ (Wilks, 2016).

2.1 Tipping points

Climate tipping points occur when a part of the climate system is in a state where a small perturbation can cause substantial qualitative alterations to the state or development of that system (Lenton et al., 2008). In section 4, we assess the MCB effect on

Table 1. Coupled CESM2 experiments used in this work

Experiment name	Configuration	Baseline Forcing	MCB forcing	Years	Ensemble Members
Historical LE	Coupled CESM2	Historical with smoothed biomass burning	None	1850 - 2014	50
SSP2-4.5 LE	Coupled CESM2	SSP2-4.5	None	2015 - 2100	17
ALL MCB	Coupled CESM2	SSP2-4.5	600cm ⁻³ in NEP, SEP, SEA	2015 - 2064	3
ALL MCB rebound	Coupled CESM2	SSP2-4.5	None	2065 - 2074	3
NEP	Coupled CESM2	SSP2-4.5	600cm ⁻³ in NEP	2015 - 2064	3
SEP	Coupled CESM2	SSP2-4.5	600cm ⁻³ in SEP	2015 - 2064	3
SEA	Coupled CESM2	SSP2-4.5	600cm ⁻³ in SEA	2015 - 2064	3

regional climate metrics associated with 14 of the tipping points identified by McKay et al. (2022) (tipping point metrics - TPM). The definitions for these TPMs are discussed in section S1 and outlined in table S1. Owing to difficulties in process representation, there is significant uncertainty among ESMs in the representation of tipping points (Drijfhout et al., 2015). Like many ESMs, CESM2 does not represent processes that drive certain tipping points. For example, the configuration used here does not include dynamic ice sheets, nor does it include dynamic forest cover (a key factor in Amazon and Sahel feedbacks). Furthermore, many tipping points occur at temperature thresholds above the warming induced under SSP2-4.5 up to 2065 (McKay et al., 2022). Thus, the TPM changes herein can only be interpreted as the tendency of anthropogenic GHG emissions to instigate a tipping point and the effect of MCB interventions on that tendency, as direct assessments of tipping point risks are largely not possible. Nevertheless, assessing the relative effects of MCB interventions on these key regional climate indicators provides insight into the benefits and risks associated with different MCB intervention strategies.

3 Results

The global mean temperature (GMST) and precipitation (GMPR) effects of 600cm^{-3} MCB interventions are shown in Fig. 1b, c. For the 2020 to 2060 average, we find that the ALL MCB forcing in CESM2 causes a $-1.05 \pm 0.02\text{K}$ (2-standard error uncertainty) GMST cooling relative to SSP2-4.5. Like Jones et al. (2009) and Hill and Ming (2012), we find that SEP forcing is the largest driver of cooling at $-0.77 \pm 0.02\text{K}$ in CESM2. However, we find relatively weaker NEP ($-0.20 \pm 0.02\text{K}$) and SEA ($-0.02 \pm 0.02\text{K}$), than these previous studies. The sum of GMST effects from the three regions is $-0.98 \pm 0.04\text{K}$. Thus, there is a modest, but nevertheless statistically significant non-linearity in the global cooling effects. Because the areal extent and ERF of each region is similar, the divergent GMST cooling suggests large differences in temperature sensitivity to MCB forcing in each region (NEP: $0.31 \pm 0.05\text{Km}^2/\text{W}$; SEP: $1.03 \pm 0.07\text{Km}^2/\text{W}$; SEA: $0.04 \pm 0.08\text{Km}^2/\text{W}$).

The ALL MCB intervention decreases GMPR by $0.088 \pm 0.001\text{mm/day}$. Thus, there is a higher sensitivity of GMPR to GMST for MCB compared to SSP2-4.5 warming (-0.087mm/day/K for ALL MCB vs. 0.061mm/day/K for SSP2-4.5). In this sense, MCB is similar to other shortwave scattering forcing such as historical tropospheric sulphate aerosol emissions (Andrews et al., 2010; Samset et al., 2016; Myhre et al., 2017) and strato-

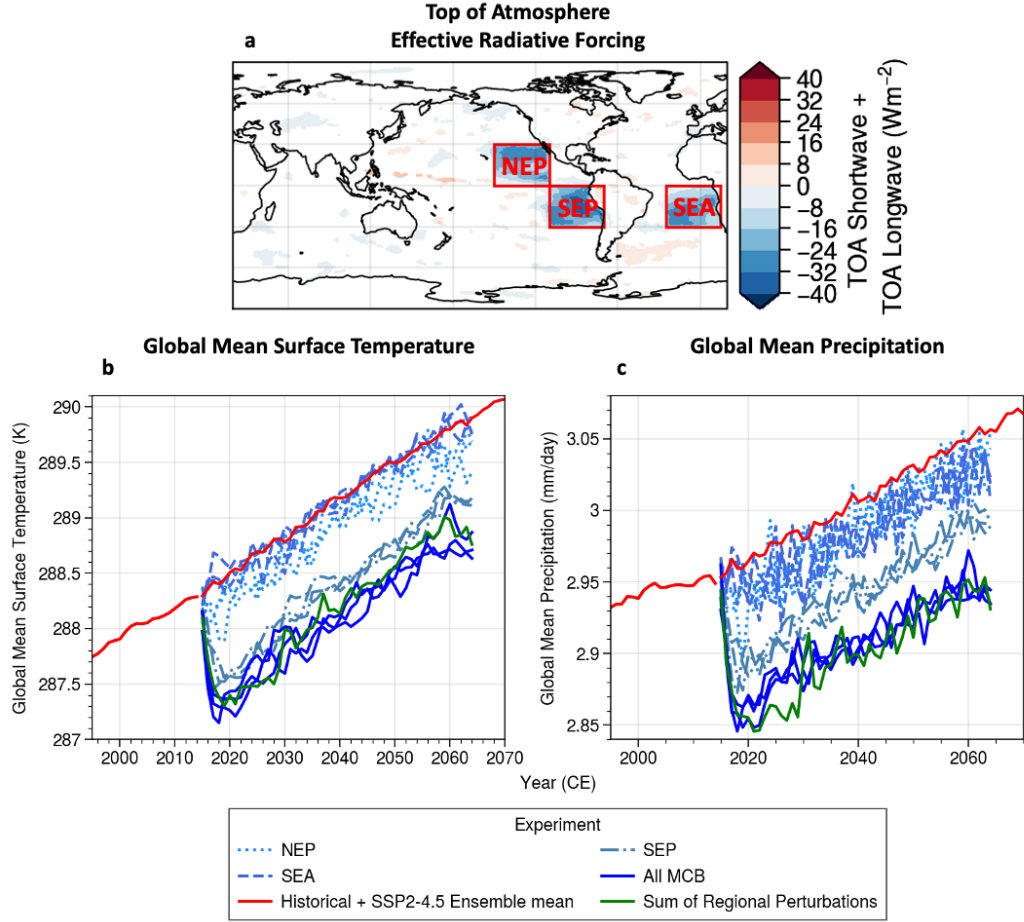


Figure 1. Map of annual mean top of atmosphere (TOA) net radiative flux (a) NEP, SEP, and SEA region definitions are shown in red boxes (non significant grid points are masked in white, $p > p_{fdr} = 0.007$). Global annual mean surface temperature (b) and precipitation (c) in the CESM2 historical and SSP2-4.5 experiments (red) and SSP2-4.5 + MCB experiments (blue shades). Ensemble mean values are shown for the historical and SSP2-4.5 ensembles while individual ensemble members are shown for the MCB experiments. Solid blue lines show the ALL MCB effect, dotted blue lines show the NEP effect, dash-dotted lines show the SEP effect, and dashed lines show the SEA effect. The solid green line shows the sum anomaly due to each region individually plus SSP2-4.5.

spheric aerosol injections (Tilmes et al., 2013; Duan et al., 2018). The GMPR response is less heavily dominated by SEP forcing than GMST. NEP and SEA forcing cause $-0.019 \pm 0.003 \text{ mm/day}$ and $-0.020 \pm 0.002 \text{ mm/day}$ drying respectively compared to $-0.055 \pm$

0.002mm/day for SEP. Thus, the GMPR sensitivity is regionally dependent, with SEA in particular causing drying in spite of a near-zero GMST effect.

3.1 Regional Climate Response to MCB Intervention

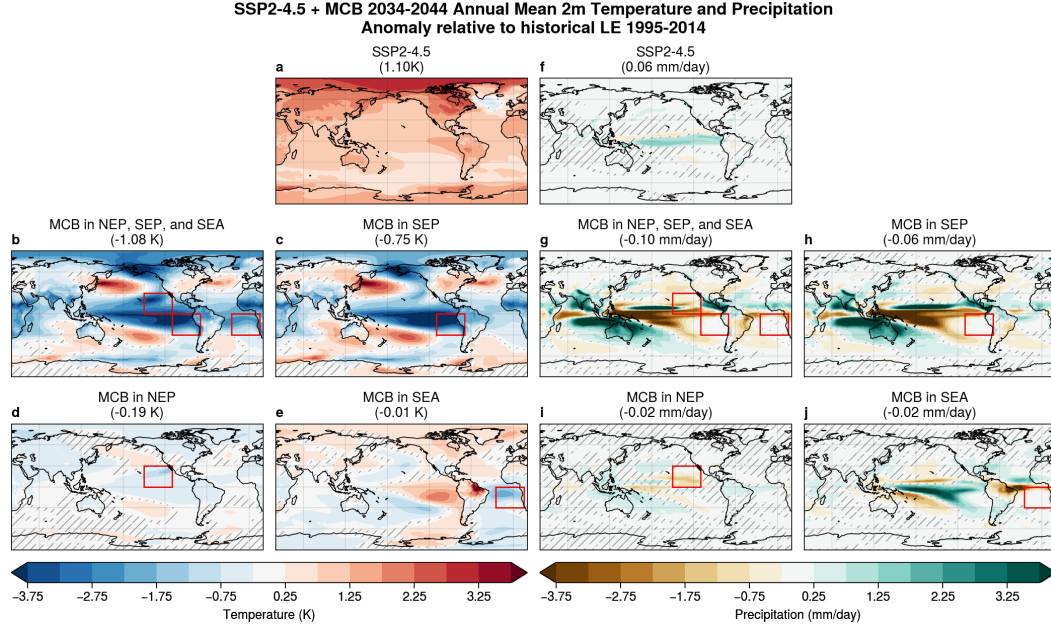


Figure 2. Maps of annual mean 2m temperature (left side: a-e) and precipitation (right side: f-j) anomalies in CESM2 SSP2-4.5 and MCB experiments for 2034-2044 relative to the CESM2 historical 1995-2015 baseline. The panels shown the SSP2-4.5 forcing response (a,f) and the MCB response for ALL MCB (b,g), SEP (c,h), NEP (d,i), and SEA (e,j). Red boxes indicate the regions in which MCB forcing is applied in each case. Global mean anomalies are shown in parentheses above each panel. Non-significant points are denoted by gray hatching. $p_{fdr} > 0.05$ for all cases.

In the following analysis (Fig. 2, Fig. 3), we compute the SSP2-4.5 response in 2034-2044 relative to the 1995-2015 historical mean. We compare this to the MCB response, the difference between the MCB and the SSP2-4.5 experiments for 2034-2044. This decade is chosen as it is the period where ALL MCB GMST cooling is approximately equal and opposite to the SSP2-4.5 warming since the baseline historical 1995-2014 mean (GMST anomalies in titles of Fig. 2a,b). Our experiments indicate that ALL MCB forcing would induce temperature anomalies that strongly resemble composite La Niña SST anoma-

lies (NOAA Physical Science Laboratory, 2023) with tropical Pacific cooling and warming in regions such as the Kuroshio and Gulf stream extensions (Fig. 2b).

The SEP experiment shows a strong La Niña-like response pattern, indicating the ALL MCB effect is mainly due to SEP MCB (Fig. 2c). The NEP experiment shows cooling in the NH generally except for warming in patches of the midlatitude North and South Pacific (Fig. 2d). The SEA experiment shows cooling in the tropical Atlantic (2e) and warming in the tropical east Pacific, northern South America, and the northern hemisphere (NH) generally. Thus, in CESM2, the interventions tested here amplify SSP2-4.5 warming in certain regions. Conversely, there are many regions where MCB cooling is stronger than SSP2-4.5 warming when the GMST responses are equal and opposite, resulting in colder conditions than the historical baseline.

The ALL MCB precipitation response also resembles La Niña composite (again primarily due to the SEP forcing; see Fig. 2h), with strong tropical Pacific drying and wetting on the poleward flanks of the Pacific and Indian ocean inter-tropical convergence zones (ITCZ). Over land, the SEP experiment shows wetting in Australian, South and East Asian, and West African monsoon regions and drying in tropical central Africa and midlatitude regions such as North America, Europe, southern Africa, and southern South America. The NEP experiment shows drying locally in the NEP forcing region and over North America and Europe (Fig. 2i). The SEA experiment shows a northward shift of the ITCZ in the Atlantic, with drying in the south of the equator and in the Amazon and wetting north of the equator and in West Africa (Fig. 2j). There is also wetting in the tropical Pacific and drying in poleward flanks of the ITCZ.

The CESM2 responses here bear broad qualitative similarities to previous HadGEM2 results (Jones et al., 2009), such as the SEP La Niña-like response and SEA Amazon drying. However, we also see key differences that indicate inter-model uncertainty in the teleconnections that drive remote climate responses to MCB. For example, the midlatitude warming, central African drying, and land monsoon wetting signals in the CESM2 SEP response are absent or much weaker in HadGEM2. Furthermore, north and tropical Pacific cooling due to NEP is weaker in CESM2 versus HadGEM2. These discrepancies are partially due to differences in forcing region definitions and forcing amount. However, the MCB ERF applied in this study is similar to Jones et al. (2009) and thus ERF differences are unlikely to account for the bulk of the differences in response.

3.2 Tipping Point Metric Response to MCB Intervention

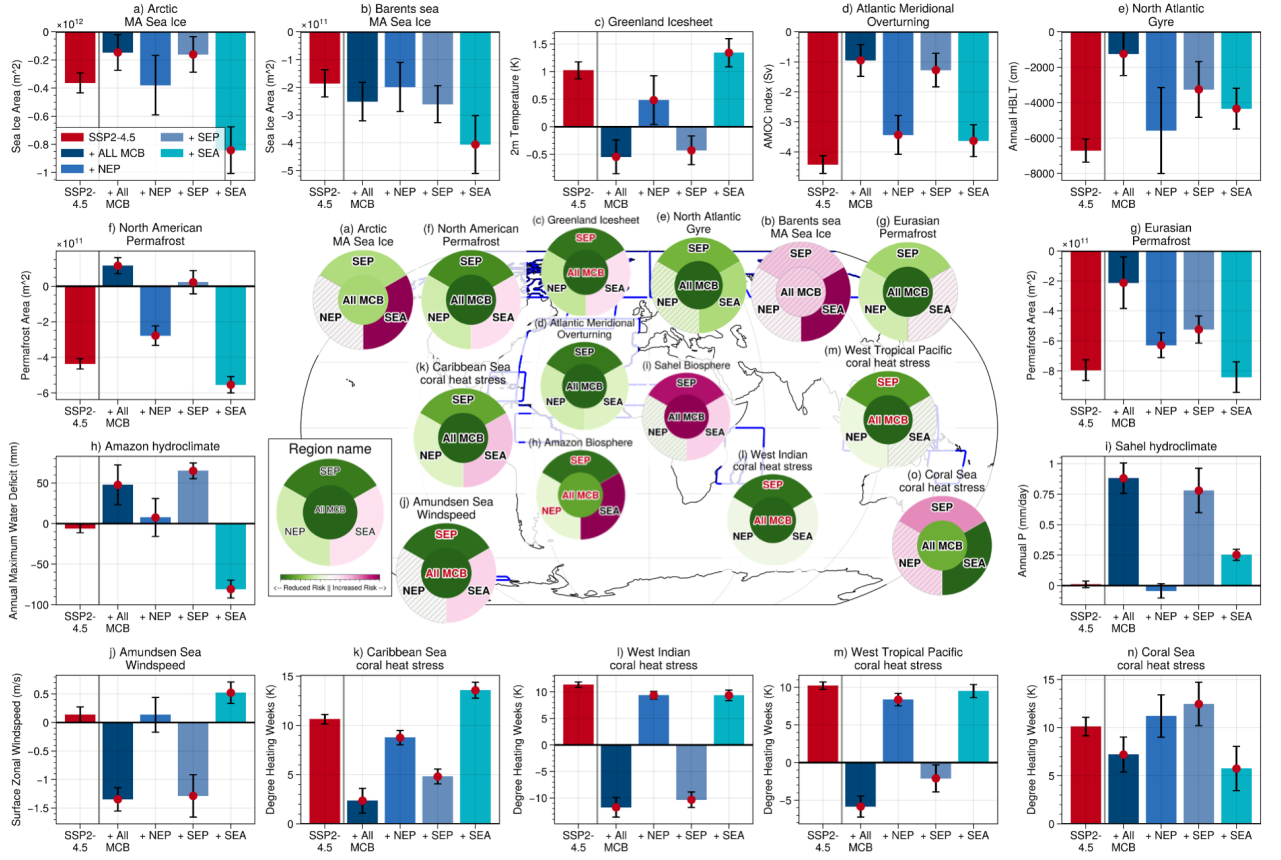


Figure 3. SSP2-4.5 and MCB impacts on tipping point metrics. Bar plots around the edge of the figure (a-o) show the 2034-2044 minus 1995-2014 anomalies for each TPM (described in Table S1) for SSP2-4.5 (red bar) and SSP2-4.5 + MCB (blue bars - from left to right: ALL MCB, NEP, SEP, and SEA). Error bars indicate the two standard error range and red dots on blue MCB bars indicate cases where the MCB effect is statistically significant using the Student's t-test ($p < 0.05$). The centre panel shows colour wheels displaying the direction of MCB impacts on each tipping element. Pink indicates a shift toward a tipping point and green indicates a shift away from it. MCB impact of SEP, NEP, and SEA (top - SEP, bottom left - NEP, bottom right - SEA) are shown in the outer wheel and the ALL MCB impact is shown in the centre circle. The colour scale of each wheel is scaled to the maximum anomaly of the four MCB experiments. Hatching indicates where MCB effects are not statistically significant at the $p < 0.05$ level. Red text labels indicate where MCB overcorrects the SSP2-4.5 effect (effect greater than and opposite to SSP2-4.5).

Fig. 3 shows the impact of SSP2-4.5 and MCB forcing on selected climate TPMs for the 2034-2044 period relative to 1995-2014. SSP2-4.5 experiments show significant changes to the selected TPMs that indicate increased tipping risk in all cases except for Sahel precipitation (Fig. 3i). The weak Sahel precipitation effect is likely a model dependent signal, as there is model uncertainty regarding the sign of the GHG precipitation impact in the region (Gaetani et al., 2017; Monerie et al., 2020).

The ALL MCB cooling results in statistically significant TPM changes that indicate reduced risk for most temperature related tipping points. Our experiments show reduced Arctic winter sea ice loss (Fig. 3a), Greenland warming (Fig. 3c), Eurasian/North American permafrost loss (Fig. 3g, f), and coral heat stress in the Caribbean sea (Fig. 3k), West Indian ocean (Fig. 3l), West Tropical Pacific (Fig. 3m) and Coral sea (Fig. 3o). We also find significant circulation responses with reduced Amundsen sea zonal wind speed (Fig. 3j), indicating reduced West Antarctic ice sheet melt, and increased AMOC index (Fig. 3d), indicating reduced AMOC collapse risk. Furthermore, contrasting the GMPR decrease, we see reductions in Amazon water deficit (Fig. 3h), indicating reduced Amazon rainforest drought risk. However, the ALL MCB experiment shows negligible effects on Barents Sea winter sea ice area (Fig. 3b) and an increase in Sahel rainfall (Fig. 3i), indicating an increased Sahel greening risk. Due to the differing climate response patterns to MCB versus GHG in our experiments, the ALL MCB does not mask the entire SSP2-4.5 signal in many regions (Fig. 3a, d, g, k, n). In others, the MCB response exceeds the GHG response (Fig. 3c, f, h, j, l, m), sometimes quite substantially, such as for Amundsen sea zonal wind speed where ALL/SEP MCB shows a strong decrease.

We find the ALL MCB changes are largely related to SEP forcing for all TPMs except Coral sea heat stress (where we see local warming; Fig. 3o). NEP forcing causes NH cooling, thus NH TPMs generally shift to indicate reduced risk, and NEP has negligible effects on TPMs in all other cases. However, the NH warming in the SEA forcing experiment drives changes that indicate increased tipping point risk many cases, as it adds to SSP2-4.5 changes for Arctic-wide and Barents winter sea ice area (Fig. 3a,b), North American permafrost (Fig. 3f), and Caribbean sea coral heat stress (Fig. 3k). Furthermore, Amazon rainfall reductions in the SEA experiment substantially increase the Amazon moisture deficit, increasing forest dieback risk (Fig. 3h), which is offset by moisture deficit decreases in the SEP and NEP experiments. On the other hand, The SEA experiment shows AMOC strengthening and reduced Coral sea heat stress, the latter of

which counteracts the warming effect of SEP forcing. Thus, SEA MCB forcing could merit further study in combination with MCB in other regions.

4 Discussion

In this study, we have conducted Community Earth System Model 2 (CESM2) experiments to explore the climate responses to Marine Cloud Brightening in three regions known for their extensive decks of marine stratus and stratocumulus clouds, with the aim of reducing the response to greenhouse gas-driven climate change. Our experiments provide a novel assessment of a key set of MCB intervention scenarios that have not been studied since CMIP3-generation models (Jones et al., 2009; Rasch et al., 2009; Hill & Ming, 2012). These scenarios are distinct from the idealized global more uniform interventions used in GeoMIP (Kravitz et al., 2013; Stjern et al., 2018), as they target regions with enhanced sensitivity to aerosol perturbations and would therefore be more efficient to brighten (Rasch et al., 2009; Latham et al., 2012). Our study reaffirms that MCB has the potential to reduce many of the climate effects of rising anthropogenic greenhouse gas concentrations. We further find that this effect extends to a range of climate indices which suggest a reduction in the risk of crossing tipping point thresholds under MCB intervention.

As noted in previous studies, the pattern and magnitude of the climate response to MCB forcing strongly depends on the location and amplitude of the intervention (Jones et al., 2009; Hill & Ming, 2012). We find qualitative agreement for many aspects of the response, although CESM2 appears more sensitive to SEP forcing and less sensitive to SEA forcing compared to models used in prior studies. Because the SEP forcing produces a response with strong similarities to La Niña anomalies, the strong SEP response may be a result of the too-strong ENSO amplitudes in CESM2 (Planton et al., 2021). The MCB pattern effect results in substantial residual regional temperature and precipitation anomalies even when the global temperature effects of SSP2-4.5 forcing and MCB are equal and opposite. Indeed, CESM2 suggests that MCB in some regions could induce (likely circulation-driven) patches of warming away from the intervention region, though this effect is less pronounced in other models (Jones et al., 2009; Hill & Ming, 2012). Thus, model representations of climate feedbacks and circulation changes play a key role in estimating the effect of MCB intervention.

It has been argued that a potential use case for SRM interventions is for rapid responses to prevent imminent climate tipping points (The Royal Society, 2009; United Nations Environment Programme, 2023). We find that MCB shows some promise in this application, as the ALL MCB intervention (forcing in all three regions considered here) causes a general shift across almost all of the TPMs we considered that indicates a reduced risk of crossing tipping point thresholds (McKay et al., 2022). However, the intervention is imperfect as the MCB pattern effect results in TPM changes that are significantly greater or less than the SSP2-4.5 effect depending on the region. Furthermore, in the case of Sahel greening, the ALL MCB intervention significantly increases rainfall in the region, increasing tipping point risk. On the other hand, over-cooling may also have negative consequences, such for coral reefs, where anomalously cold conditions can increase coral mortality (Kemp et al., 2011).

The MCB effect on TPMs is sensitive to pattern of the forcing such that some cases may exacerbate the SSP2-4.5 effect. For example, our SEA experiment shows substantially reduce rainfall in eastern Brazil, increasing the risk of drought and rainforest dieback in the region (as also noted by Jones et al. (2009)). However, we note that many of these regional effects are non-additive, such that MCB in SEA could be considered in combination with MCB in other regions. In addition, many tipping points occur in regions where ESMs have substantial biases and are subject to uncertainties in process representation (see section S1). Thus, tipping point representation presents an important uncertainty in the evaluation of SRM interventions. The prominent role of the pattern effect necessitates comprehensive assessment across different tipping elements and scenarios to evaluate MCB as an intervention option.

The MCB “pattern response” poses a significant challenge to exploring and assessing MCB as an option for climate intervention. Combined with the fact that MCB intervention could be applied over relatively small temporal and spatial scales, this significantly expands MCB scenario uncertainty and introduces additional degrees of freedom to consider when performing MCB “controller” simulations (of the kind used in SAI simulations; see Tilmes et al., 2018; Richter et al., 2022). On the other hand, the large possibility space of MCB intervention patterns leaves open the potential to identify specific MCB intervention patterns that reduce tipping point risks while minimizing unintended negative remote consequences.

Though we only assess one model here, the differences in the global mean and pattern of climate response to MCB between this and past studies suggest substantial inter-model uncertainties stemming from uncertainty in the representation of climate feedbacks and atmosphere-ocean circulation. Such uncertainties are distinct from uncertainties arising from differences in aerosol injection methods or aerosol microphysics representation. Because many of the desired responses to MCB would occur away from the forcing regions themselves, it is crucial that such circulation uncertainties are understood and reduced in order to evaluate the feasibility of MCB interventions (Diamond et al., 2022).

Our experiments model MCB perturbations by directly perturbing CDNC, which neglects the sea salt direct aerosol forcing and the effect of aerosol transport on the forcing patterns (Partanen et al., 2012; Ahlm et al., 2017). We also do not model the effect of sea salt on atmospheric chemistry (Horowitz et al., 2020). While we anticipate that the remote response to MCB interventions will be mostly insensitive to the specifics the MCB shortwave forcing in a given region, this may not necessarily be the case. Furthermore, CESM2 has among the highest aerosol-cloud interaction effects in the CMIP6 ensemble (Smith et al., 2020), meaning weaker CDNC perturbations are required to achieve a given forcing compared to other models. These issues highlight a need for systematic assessment of MCB intervention in key high susceptibility regions and their consequent climate responses. Evaluating such uncertainties will be a key aim of a forthcoming multi-model intercomparison of regional MCB applications.

Open Research Section

CESM2 code modifications and model output and analysis scripts available at Haruki Hirasawa, Dipti Swapnil Hingmire, Hansi Alice Singh, Philip J. Rasch, and Peetak Mitra. (2023). Replication data for: Effect of Regional Marine Cloud Brightening Interventions on Climate Tipping Points [Data set]. Zenodo. <https://doi.org/10.5281/zenodo.7884575>, CC BY-NC-SA 4.0. CESM2 LE historical and SSP2-4.5 data available from the National Center for Atmospheric Research <https://www.cesm.ucar.edu/community-projects/lens2/datasets>.

Acknowledgments

We thank Brian Dobbins of the National Center for Atmospheric Research and Linda Hedges of Silver Lining for their valuable technical assistance with our CESM2 simula-

tions. This work was partly funded by the DARPA AI-assisted Climate Tipping-point Modeling (ACTM) program under award DARPA-PA-21-04-02. The CESM2 simulations were performed using Amazon Web Services (AWS) thanks to a generous computing grant provided by Amazon. We thank the CESM2 Large Ensemble Community Project and the supercomputing resources provided by the IBS Center for Climate Physics in South Korea for for the CESM2 LE data used herein.

References

- Ahlm, L., Jones, A., Stjern, C. W., Muri, H., Kravitz, B., & Kristjánsson, J. E. (2017, November). Marine cloud brightening – as effective without clouds. *Atmospheric Chemistry and Physics*, 17(21), 13071–13087. Retrieved 2023-02-28, from <https://acp.copernicus.org/articles/17/13071/2017/> doi: 10.5194/acp-17-13071-2017
- Alterskjær, K., Kristjánsson, J. E., Boucher, O., Muri, H., Niemeier, U., Schmidt, H., ... Timmreck, C. (2013, November). Sea-salt injections into the low-latitude marine boundary layer: The transient response in three Earth system models. *Journal of Geophysical Research: Atmospheres*, 118(21). Retrieved 2023-03-01, from <https://onlinelibrary.wiley.com/doi/10.1002/2013JD020432> doi: 10.1002/2013JD020432
- Andrews, T., Forster, P. M., Boucher, O., Bellouin, N., & Jones, A. (2010, July). Precipitation, radiative forcing and global temperature change. *Geophysical Research Letters*, 37(14), n/a–n/a. Retrieved 2022-01-10, from <http://doi.wiley.com/10.1029/2010GL043991> doi: 10.1029/2010GL043991
- Bala, G., Caldeira, K., Nemani, R., Cao, L., Ban-Weiss, G., & Shin, H.-J. (2011, September). Albedo enhancement of marine clouds to counteract global warming: impacts on the hydrological cycle. *Climate Dynamics*, 37(5-6), 915–931. Retrieved 2023-03-01, from <http://link.springer.com/10.1007/s00382-010-0868-1> doi: 10.1007/s00382-010-0868-1
- Danabasoglu, G., Lamarque, J., Bacmeister, J., Bailey, D. A., DuVivier, A. K., Edwards, J., ... Strand, W. G. (2020, February). The Community Earth System Model Version 2 (CESM2). *Journal of Advances in Modeling Earth Systems*, 12(2). Retrieved 2022-10-14, from <https://onlinelibrary.wiley.com/doi/10.1029/2019MS001916> doi: 10.1029/2019MS001916

- 379 Diamond, M. S., Gettelman, A., Lebsock, M. D., McComiskey, A., Russell, L. M.,
380 Wood, R., & Feingold, G. (2022, January). To assess marine cloud
381 brightening’s technical feasibility, we need to know what to study—and
382 when to stop. *Proceedings of the National Academy of Sciences*, 119(4),
383 e2118379119. Retrieved 2022-07-04, from [https://pnas.org/doi/full/](https://pnas.org/doi/full/10.1073/pnas.2118379119)
384 [10.1073/pnas.2118379119](https://pnas.org/doi/full/10.1073/pnas.2118379119) doi: 10.1073/pnas.2118379119
- 385 Drijfhout, S., Bathiany, S., Beaulieu, C., Brovkin, V., Claussen, M., Hunting-
386 ford, C., ... Swingedouw, D. (2015, October). Catalogue of abrupt shifts
387 in Intergovernmental Panel on Climate Change climate models. *Proceed-*
388 *ings of the National Academy of Sciences*, 112(43). Retrieved 2023-01-
389 18, from <https://pnas.org/doi/full/10.1073/pnas.1511451112> doi:
390 [10.1073/pnas.1511451112](https://pnas.org/doi/full/10.1073/pnas.1511451112)
- 391 Duan, L., Cao, L., Bala, G., & Caldeira, K. (2018, November). Comparison of the
392 Fast and Slow Climate Response to Three Radiation Management Geoengi-
393 neering Schemes. *Journal of Geophysical Research: Atmospheres*, 123(21),
394 11,980–12,001. Retrieved 2023-03-01, from [https://onlinelibrary.wiley](https://onlinelibrary.wiley.com/doi/abs/10.1029/2018JD029034)
395 [.com/doi/abs/10.1029/2018JD029034](https://onlinelibrary.wiley.com/doi/abs/10.1029/2018JD029034) doi: 10.1029/2018JD029034
- 396 Gaetani, M., Flamant, C., Bastin, S., Janicot, S., Lavaysse, C., Hourdin, F., ...
397 Bony, S. (2017, February). West African monsoon dynamics and precipitation:
398 the competition between global SST warming and CO₂ increase in CMIP5
399 idealized simulations. *Climate Dynamics*, 48(3-4), 1353–1373. Retrieved 2022-
400 01-10, from <http://link.springer.com/10.1007/s00382-016-3146-z> doi:
401 [10.1007/s00382-016-3146-z](http://link.springer.com/10.1007/s00382-016-3146-z)
- 402 Hill, S., & Ming, Y. (2012, August). Nonlinear climate response to regional
403 brightening of tropical marine stratocumulus: CLIMATE RESPONSE TO
404 CLOUD BRIGHTENING. *Geophysical Research Letters*, 39(15). Retrieved
405 2023-03-01, from <http://doi.wiley.com/10.1029/2012GL052064> doi:
406 [10.1029/2012GL052064](http://doi.wiley.com/10.1029/2012GL052064)
- 407 Horowitz, H. M., Holmes, C., Wright, A., Sherwen, T., Wang, X., Evans, M., ...
408 Alexander, B. (2020, February). Effects of Sea Salt Aerosol Emissions for
409 Marine Cloud Brightening on Atmospheric Chemistry: Implications for Ra-
410 diative Forcing. *Geophysical Research Letters*, 47(4). Retrieved 2023-02-28,
411 from <https://onlinelibrary.wiley.com/doi/10.1029/2019GL085838> doi:

- 10.1029/2019GL085838
- Jones, A., Haywood, J., & Boucher, O. (2009, May). Climate impacts of geo-engineering marine stratocumulus clouds. *Journal of Geophysical Research: Atmospheres*, 114(D10), 2008JD011450. Retrieved 2022-09-21, from <https://onlinelibrary.wiley.com/doi/10.1029/2008JD011450> doi: 10.1029/2008JD011450
- Kemp, D. W., Oakley, C. A., Thornhill, D. J., Newcomb, L. A., Schmidt, G. W., & Fitt, W. K. (2011, November). Catastrophic mortality on inshore coral reefs of the Florida Keys due to severe low-temperature stress. *Global Change Biology*, 17(11), 3468–3477. Retrieved 2023-03-02, from <https://onlinelibrary.wiley.com/doi/10.1111/j.1365-2486.2011.02487.x> doi: 10.1111/j.1365-2486.2011.02487.x
- Korhonen, H., Carslaw, K. S., & Romakkaniemi, S. (2010, May). Enhancement of marine cloud albedo via controlled sea spray injections: a global model study of the influence of emission rates, microphysics and transport. *Atmospheric Chemistry and Physics*, 10(9), 4133–4143. Retrieved 2023-03-01, from <https://acp.copernicus.org/articles/10/4133/2010/> doi: 10.5194/acp-10-4133-2010
- Kravitz, B., Forster, P. M., Jones, A., Robock, A., Alterskjaer, K., Boucher, O., ... Watanabe, S. (2013, October). Sea spray geoengineering experiments in the geoengineering model intercomparison project (GeoMIP): Experimental design and preliminary results: GEOMIP MARINE CLOUD BRIGHTENING. *Journal of Geophysical Research: Atmospheres*, 118(19), 11,175–11,186. Retrieved 2022-01-10, from <http://doi.wiley.com/10.1002/jgrd.50856> doi: 10.1002/jgrd.50856
- Kravitz, B., Robock, A., Tilmes, S., Boucher, O., English, J. M., Irvine, P. J., ... Watanabe, S. (2015, October). The Geoengineering Model Intercomparison Project Phase 6 (GeoMIP6): simulation design and preliminary results. *Geoscientific Model Development*, 8(10), 3379–3392. Retrieved 2022-01-10, from <https://gmd.copernicus.org/articles/8/3379/2015/> doi: 10.5194/gmd-8-3379-2015
- Latham, J. (2002). Amelioration of global warming by controlled enhancement of the albedo and longevity of low-level maritime clouds. *Atmospheric Science*

- Letters, 3(2-4), 42–51. Retrieved 2023-03-01, from <http://doi.wiley.com/10.1006/asle.2002.0099> doi: 10.1006/asle.2002.0099
- Latham, J., Bower, K., Choularton, T., Coe, H., Connolly, P., Cooper, G., ... Wood, R. (2012, September). Marine cloud brightening. *Philosophical Transactions of the Royal Society A: Mathematical, Physical and Engineering Sciences*, 370(1974), 4217–4262. Retrieved 2022-04-04, from <https://royalsocietypublishing.org/doi/10.1098/rsta.2012.0086> doi: 10.1098/rsta.2012.0086
- Latham, J., Rasch, P., Chen, C.-C., Kettles, L., Gadian, A., Gettelman, A., ... Choularton, T. (2008, November). Global temperature stabilization via controlled albedo enhancement of low-level maritime clouds. *Philosophical Transactions of the Royal Society A: Mathematical, Physical and Engineering Sciences*, 366(1882), 3969–3987. Retrieved 2023-01-05, from <https://royalsocietypublishing.org/doi/10.1098/rsta.2008.0137> doi: 10.1098/rsta.2008.0137
- Lenton, T. M., Held, H., Kriegler, E., Hall, J. W., Lucht, W., Rahmstorf, S., & Schellnhuber, H. J. (2008, February). Tipping elements in the Earth’s climate system. *Proceedings of the National Academy of Sciences*, 105(6), 1786–1793. Retrieved 2023-04-17, from <https://pnas.org/doi/full/10.1073/pnas.0705414105> doi: 10.1073/pnas.0705414105
- McKay, D. I. A., Staal, A., Abrams, J. F., Winkelmann, R., Sakschewski, B., Loriani, S., ... Lenton, T. M. (2022). Exceeding 1.5°C global warming could trigger multiple climate tipping points. *Science*, 377, 6611. doi: 10.1126/science.abn7950
- Meinshausen, M., Lewis, J., McGlade, C., Gütschow, J., Nicholls, Z., Burdon, R., ... Hackmann, B. (2022, April). Realization of Paris Agreement pledges may limit warming just below 2 °C. *Nature*, 604(7905), 304–309. Retrieved 2022-10-14, from <https://www.nature.com/articles/s41586-022-04553-z> doi: 10.1038/s41586-022-04553-z
- Monerie, P.-A., Wainwright, C. M., Sidibe, M., & Akinsanola, A. A. (2020, September). Model uncertainties in climate change impacts on Sahel precipitation in ensembles of CMIP5 and CMIP6 simulations. *Climate Dynamics*, 55(5-6), 1385–1401. Retrieved 2022-01-10, from <https://link.springer.com/>

- 10.1007/s00382-020-05332-0 doi: 10.1007/s00382-020-05332-0
- Muri, H., Tjiputra, J., Otterå, O. H., Adakudlu, M., Lauvset, S. K., Grini, A., ... Kristjánsson, J. E. (2018, August). Climate Response to Aerosol Geoengineering: A Multimethod Comparison. *Journal of Climate*, 31(16), 6319–6340. Retrieved 2023-03-01, from <https://journals.ametsoc.org/doi/10.1175/JCLI-D-17-0620.1> doi: 10.1175/JCLI-D-17-0620.1
- Myhre, G., Forster, P. M., Samset, B. H., Hodnebrog, , Sillmann, J., Aalbergstjø, S. G., ... Zwiers, F. (2017, June). PDRMIP: A Precipitation Driver and Response Model Intercomparison Project—Protocol and Preliminary Results. *Bulletin of the American Meteorological Society*, 98(6), 1185–1198. Retrieved 2022-01-10, from <https://journals.ametsoc.org/doi/10.1175/BAMS-D-16-0019.1> doi: 10.1175/BAMS-D-16-0019.1
- National Academies of Sciences, Engineering, and Medicine. (2021). *Reflecting Sunlight: Recommendations for Solar Geoengineering Research and Research Governance*. Washington, D.C.: National Academies Press. Retrieved 2023-04-05, from <https://www.nap.edu/catalog/25762> (Pages: 25762) doi: 10.17226/25762
- NOAA Physical Science Laboratory. (2023). *El Niño Southern Oscillation (ENSO)*. Retrieved 2023-03-01, from <https://psl.noaa.gov/enso/>
- Partanen, A.-I., Kokkola, H., Romakkaniemi, S., Kerminen, V.-M., Lehtinen, K. E. J., Bergman, T., ... Korhonen, H. (2012, January). Direct and indirect effects of sea spray geoengineering and the role of injected particle size: SEA SPRAY GEOENGINEERING. *Journal of Geophysical Research: Atmospheres*, 117(D2), n/a–n/a. Retrieved 2023-03-01, from <http://doi.wiley.com/10.1029/2011JD016428> doi: 10.1029/2011JD016428
- Planton, Y. Y., Guilyardi, E., Wittenberg, A. T., Lee, J., Gleckler, P. J., Bayr, T., ... Voldoire, A. (2021, February). Evaluating Climate Models with the CLIVAR 2020 ENSO Metrics Package. *Bulletin of the American Meteorological Society*, 102(2), E193–E217. Retrieved 2022-10-14, from <https://journals.ametsoc.org/view/journals/bams/102/2/BAMS-D-19-0337.1.xml> doi: 10.1175/BAMS-D-19-0337.1
- Rasch, P. J., Latham, J., & Chen, C.-C. J. (2009, October). Geoengineering by cloud seeding: influence on sea ice and climate system. *Envi-*

- 511 *ronmental Research Letters*, 4(4), 045112. Retrieved 2022-08-09, from
512 <https://iopscience.iop.org/article/10.1088/1748-9326/4/4/045112>
513 doi: 10.1088/1748-9326/4/4/045112
- 514 Richter, J. H., Visionsi, D., MacMartin, D. G., Bailey, D. A., Rosenbloom, N., Dob-
515 bins, B., ... Lamarque, J.-F. (2022, November). Assessing Responses and
516 Impacts of Solar climate intervention on the Earth system with stratospheric
517 aerosol injection (ARISE-SAI): protocol and initial results from the first sim-
518 ulations. *Geoscientific Model Development*, 15(22), 8221–8243. Retrieved
519 2023-02-28, from <https://gmd.copernicus.org/articles/15/8221/2022/>
520 doi: 10.5194/gmd-15-8221-2022
- 521 Rodgers, K. B., Lee, S.-S., Rosenbloom, N., Timmermann, A., Danabasoglu, G.,
522 Deser, C., ... Yeager, S. G. (2021, December). Ubiquity of human-induced
523 changes in climate variability. *Earth System Dynamics*, 12(4), 1393–1411. Re-
524 trieved 2022-12-09, from [https://esd.copernicus.org/articles/12/1393/](https://esd.copernicus.org/articles/12/1393/2021/)
525 2021/ doi: 10.5194/esd-12-1393-2021
- 526 Samset, B. H., Myhre, G., Forster, P. M., Hodnebrog, , Andrews, T., Faluvegi,
527 G., ... Voulgarakis, A. (2016, March). Fast and slow precipitation re-
528 sponses to individual climate forcings: A PDRMIP multimodel study. *Geo-*
529 *physical Research Letters*, 43(6), 2782–2791. Retrieved 2022-01-10, from
530 <https://onlinelibrary.wiley.com/doi/abs/10.1002/2016GL068064> doi:
531 10.1002/2016GL068064
- 532 Smith, C. J., Kramer, R. J., Myhre, G., Alterskjær, K., Collins, W., Sima, A., ...
533 Forster, P. M. (2020, August). Effective radiative forcing and adjustments in
534 CMIP6 models. *Atmospheric Chemistry and Physics*, 20(16), 9591–9618. Re-
535 trieved 2023-04-05, from [https://acp.copernicus.org/articles/20/9591/](https://acp.copernicus.org/articles/20/9591/2020/)
536 2020/ doi: 10.5194/acp-20-9591-2020
- 537 Smith, C. J., Kramer, R. J., Myhre, G., Forster, P. M., Soden, B. J., Andrews, T.,
538 ... Watson-Parris, D. (2018, November). Understanding Rapid Adjustments to
539 Diverse Forcing Agents. *Geophysical Research Letters*, 45(21). Retrieved 2023-
540 04-04, from <https://onlinelibrary.wiley.com/doi/10.1029/2018GL079826>
541 doi: 10.1029/2018GL079826
- 542 Stjern, C. W., Muri, H., Ahlm, L., Boucher, O., Cole, J. N. S., Ji, D., ...
543 Kristjánsson, J. E. (2018, January). Response to marine cloud brightening

544 in a multi-model ensemble. *Atmospheric Chemistry and Physics*, 18(2), 621–
545 634. Retrieved 2022-09-16, from [https://acp.copernicus.org/articles/18/](https://acp.copernicus.org/articles/18/621/2018/)
546 621/2018/ doi: 10.5194/acp-18-621-2018

547 Stuart, G. S., Stevens, R. G., Partanen, A.-I., Jenkins, A. K. L., Korhonen, H.,
548 Forster, P. M., ... Pierce, J. R. (2013, October). Reduced efficacy of marine
549 cloud brightening geoengineering due to in-plume aerosol coagulation: pa-
550 rameterization and global implications. *Atmospheric Chemistry and Physics*,
551 13(20), 10385–10396. Retrieved 2023-03-01, from [https://acp.copernicus](https://acp.copernicus.org/articles/13/10385/2013/)
552 [.org/articles/13/10385/2013/](https://acp.copernicus.org/articles/13/10385/2013/) doi: 10.5194/acp-13-10385-2013

553 The Royal Society. (2009). *Geoengineering the climate: science, governance and un-*
554 *certainty*. London: Royal Society. (OCLC: 436232805)

555 Tilmes, S., Fasullo, J., Lamarque, J.-F., Marsh, D. R., Mills, M., Alterskjaer, K.,
556 ... Watanabe, S. (2013, October). The hydrological impact of geoengineer-
557 ing in the Geoengineering Model Intercomparison Project (GeoMIP): THE
558 HYDROLOGIC IMPACT OF GEOENGINEERING. *Journal of Geophysical*
559 *Research: Atmospheres*, 118(19), 11,036–11,058. Retrieved 2023-03-21, from
560 <http://doi.wiley.com/10.1002/jgrd.50868> doi: 10.1002/jgrd.50868

561 Tilmes, S., Richter, J. H., Kravitz, B., MacMartin, D. G., Mills, M. J., Simpson,
562 I. R., ... Ghosh, S. (2018, November). CESM1(WACCM) Stratospheric
563 Aerosol Geoengineering Large Ensemble Project. *Bulletin of the American Me-*
564 *teorological Society*, 99(11), 2361–2371. Retrieved 2023-04-05, from [https://](https://journals.ametsoc.org/view/journals/bams/99/11/bams-d-17-0267.1.xml)
565 journals.ametsoc.org/view/journals/bams/99/11/bams-d-17-0267.1.xml
566 doi: 10.1175/BAMS-D-17-0267.1

567 Tilmes, S., Richter, J. H., Mills, M. J., Kravitz, B., MacMartin, D. G., Vitt, F.,
568 ... Lamarque, J. (2017, December). Sensitivity of Aerosol Distribution
569 and Climate Response to Stratospheric SO₂ Injection Locations. *Journal*
570 *of Geophysical Research: Atmospheres*, 122(23). Retrieved 2023-03-01, from
571 <https://onlinelibrary.wiley.com/doi/10.1002/2017JD026888> doi:
572 10.1002/2017JD026888

573 United Nations Environment Programme. (2023). *One Atmosphere: An Indepen-*
574 *dent Expert Review on Solar Radiation Modification Research and Deployment*.
575 Kenya, Nairobi. Retrieved from [https://wedocs.unep.org/20.500.11822/](https://wedocs.unep.org/20.500.11822/41903)
576 41903

- 577 Wilks, D. S. (2016, December). “The Stippling Shows Statistically Signifi-
578 cant Grid Points”: How Research Results are Routinely Overstated and
579 Overinterpreted, and What to Do about It. *Bulletin of the American*
580 *Meteorological Society*, 97(12), 2263–2273. Retrieved 2022-01-10, from
581 <https://journals.ametsoc.org/doi/10.1175/BAMS-D-15-00267.1> doi:
582 10.1175/BAMS-D-15-00267.1
- 583 Wood, R. (2021, October). Assessing the potential efficacy of marine cloud
584 brightening for cooling Earth using a simple heuristic model. *Atmo-*
585 *spheric Chemistry and Physics*, 21(19), 14507–14533. Retrieved 2022-06-
586 27, from <https://acp.copernicus.org/articles/21/14507/2021/> doi:
587 10.5194/acp-21-14507-2021